404–416 Vol. 78 No. 2 ACTA GEOLOGICA SINICA April 2004
http://www.geojournals.cn/dzxbcn/ch/index.aspx

The Bulong Gold Deposit—a Quartz-Barite Vein Type Gold Deposit in Xinjiang: Geological Characteristics and S, He and Ar Isotopic Compositions

YANG Fuquan, WANG Yitian and MAO Jingwen
Institute of Mineral Resources, Chinese Academy of Geological Sciences, Beijing 100037;
E-mail: Yangfuquan66@sina.com

Abstract The Bulong gold deposit, located in the southwest Tianshan in China, occurs in the Upper Devonian fine-grained clastic rocks. The gold orebodies are controlled by an gently inclined interlayer fractured zone. They are hosted only in quartz-barite veins though there are barite veins and quartz veins in the ore district. The $\delta^{34}S$ values of pyrite in the ores range from 14.6‰ to 19.2‰ and those of barite from 35.0‰ to 39.6‰, indicating that the sulfur was derived from the strata. $^{3}He/^{4}He$ ratios of fluid inclusions in pyrite are 0.24–0.82 R/Ra, approximating to that of the crust. The $^{40}Ar/^{36}Ar$ ratios range from 338 to 471, slightly higher than that of the atmosphere. $^{40}Ar/^{4}He$ ratios of ore fluids range from 0.015 to 0.412 with a mean of 0.153. Helium and argon isotope compositions of fluid inclusions show that the ore fluids of the Bulong gold deposit were mainly derived from the crust.

Key words: quartz-barite vein type gold deposit, geology of deposit, sulfur, helium and argon isotopes, Bulong, Xinjiang

1 Introduction

The southern Tianshan antimony-mercury-gold metallogenic belt in Central Asia is one of the important gold belts in the world, and the southwestern Tianshan Mountains in Xinjiang are its eastward extension, where the Sawayaerdun, Dashankou, Sahentuohai and Bulong gold deposits have been discovered in recent years, implying good ore-hunting prospects in this area. The Bulong gold deposit is a new type gold deposit—a quartz-barite vein type deposit, which was discovered by the No. 8 Geological Party, Xinjiang Bureau of Geology and Mineral Exploration and Development at the beginning of the 1990s, and inspecting, appraising and geological reconnaissance were carried out in 1994 and 1999. The gold reserves of the Bulong deposit are ca. 1 ton, and both gold and barite are being mined at present at a small scale. The Bulong gold deposit is less studied (Yang and Wu, 1999; Yang et al., 1999; Ye et al., 1999). The systematic study of the metallogenic characteristics, ore-forming materials and ore-forming fluid source of this rare type of gold deposit, as well as its unique metallogenesis is of great significance. Therefore, the source of the ore-forming fluids of the Bulong gold deposit is studied through the stable isotope and inert gas isotope geochemistry in this paper.

2 Regional Geology

The Bulong gold deposit is situated at Bulong Village, 43 km southwest of Akqi County, Kizilsu Kirgiz Autonomous Prefecture, Xinjiang. Its geographical coordinates are 77°56′00″ – 77°59′30″E and 40°48′00″ – 40°50′30″N. Tectonically, the Bulong deposit is located in a mobile belt on the northern margin of the Tarim plate, on the southeastern side of the regional NE-trending Karateki fault, which separates the Late Palaeozoic southern Tianshan epicontinental basin from the Palaeozoic Kalpin foreland basin.

The strata exposed in the southeastern ore district are the Silurian and Upper Devonian Yimugantawu Formation and Kiziltag Formation and the Upper Carboniferous Kangkelin Formation. The Silurian is distributed in the southeastern part of the area and composed of low-grade metamorphic sandstone, siltstone and mudstone. The Upper Devonian Yimugantawu Formation is exposed in the central part of the ore district (Fig. 1), represented by a suite of purplish red and deep red, thin- to medium-bedded quartz siltstone and quartz fine sandstone and greyish green, thin-bedded siltstone, intercalated with mudstone and shale and locally intercalated with thin-bedded conglomerate, showing the features of the flysch formation. The rocks have been phyllitic and schistose. The quartz-barite type gold veins are dominantly hosted in this formation. The Upper Devonian Kiziltag Formation is a sequence of brick-red phyllitized quartz sandstone and siltstone intercalated with white quartz sandstone and locally intercalated with sandstone-conglomerate and shale, and oblique bedding and ripple marks are well developed. Some barite veins and most gold-bearing quartz

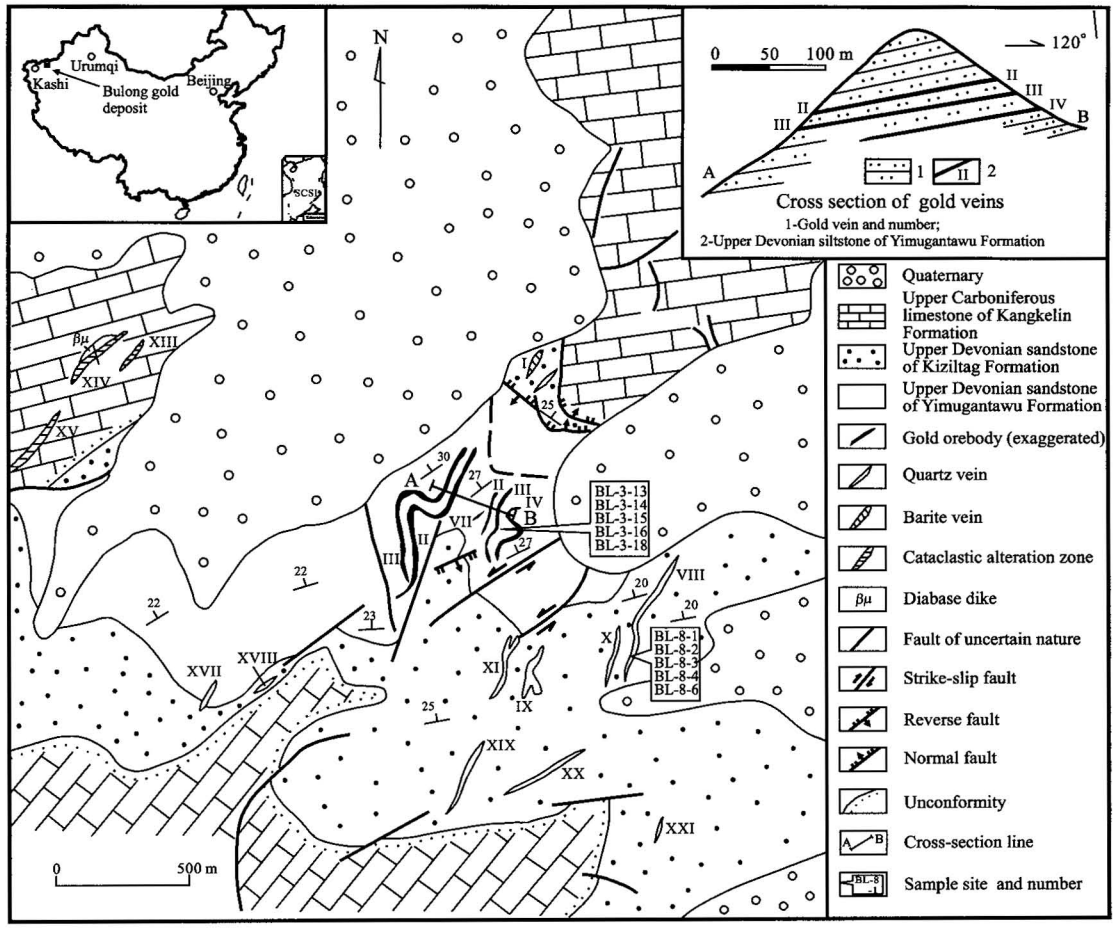

Fig. 1. Geological sketch map of the Bulong gold deposit (after No. 8 Geological Party, Xinjiang Bureau of Geology and Mineral Exploration and Development, 1999).

veins are hosted in this formation. The Upper Carboniferous Kangkelin Formation is a sequence of grey, dark grey, massive to thick-bedded limestone and greyish black, thin- to medium-bedded limestone, locally intercalated with sandstone, siltstone and shale. Three cataclastic alteration zones are found in the strata, but no gold mineralization is present.

The ore district is located in the northwestern limb of the Aerbaqieke box anticline. The Karateki fault is long-active, large in scale and deep. The ore veins are controlled by the NE-trending, interlayer, gently inclined fracture zones.

No magmatic rocks are exposed in the ore district, except for a few diabase and diabase-porphyrite dykes in the western part of the ore district and its surroundings, which are several to a few hundred meters long and tens of centimeters to several meters wide.

3 Geology of Ore Deposit

3.1 Ore veins

More than 20 auriferous quartz-barite veins, quartz veins, barite veins and cataclastic alteration zones have been found in the Bulong ore district (Fig. 1). Among them, No. I vein is a barite vein, occurring in a fracture zone in the Upper Devonian Kiziltag Formation in the northern part of the ore district. It trends NNE and intersects obliquely with the strata at a high angle. The barite vein is fractured, with rare sulphide, and its average gold grade is 0.45 g/t. Nos. II, III and IV ore veins are gold-bearing quartz-barite veins, and their basic features are shown in Table 1. These three veins are parallel to each other and ~20–50 m apart. They dip 320°–10° at 10°–28°, being largely concordant with the bedding of the strata. In plan views, they meander in a NE direction. Branching and converging may be found locally for No. III ore vein. The branches are barite veins, 10–50 cm thick, which are distributed along fissures and obviously cut through the strata. Nos. II and III ore veins are exposed on both sides of a ridge (cross section in Fig. 1). The auriferous quartz-barite veins have well-defined boundaries with the wall rocks. They are dominantly pure barite veins, quartz veins, quartz-barite veins and some calcite-quartz-barite veins. In

vertical section (Fig. 2), we can see pure barite veins in the middle and quartz veins or barite-quartz veins in the lower and upper parts, with thicknesses of 5–40 cm. The gold orebodies mainly occur as quartz veins and quartz-barite veins. The orebodies appear as gently inclined thin beds, whose size is notably smaller than the compound veins in which they are hosted (Table 1). The average gold grade is 1.64–3.72 g/t, and the gold grade of ores in No. II orebody ranges from 1.13 to 7.45 g/t, with a maximum of 18.03 g/t and a mean of 3.72 g/t.

No. VII orebody, cataclastic and brecciated, occurs in a barite-bearing quartz vein. It is the smallest one in the deposit, characterized by the presence of abundant visible gold. Tens of gold grains can be observed in a hand specimen 6×4×3 cm^3 in size.

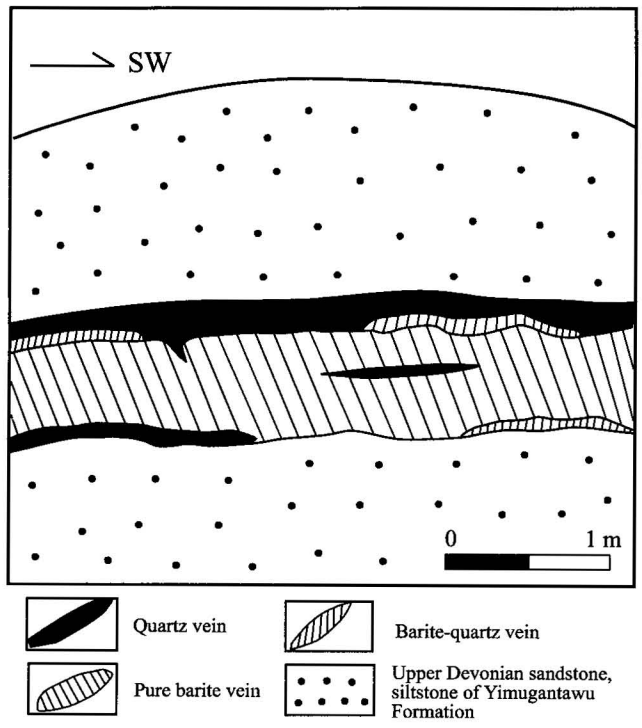

Fig. 2. Schematic cross section of No III ore vein.

Nos. VIII–XI and XVII–XXI veins are large quartz veins, which occur in the Kizirtag Formation in the southern part of the ore district. The veins trend NNE and NE, obviously striking obliquely to the strike of the strata; they dip steeply at angles of more than 60°. Minor pyritization is developed in the veins, and the gold grade is low, being < 0.5 g/t, and in a few cases the grade may reach 1.04–5.77 g/t. Gold is of very uneven distribution. Gold mineralization of Nos. X and XI veins is relatively good but of no economic value. No. VIII vein, nearly upright, is the largest one among the quartz veins, being 450 m long and 0.8–5.0 m thick, and the highest gold grade is up to 3.08 g/t. No. XI vein is 250 m in length and 0.3–1.2 m in thickness, whose gold grade is about 0.1–0.48 g/t with a maximum of 0.96 g/t. The rest large quartz veins are generally 100–300 m long and 0.5–3.0 m thick.

3.2 Mineralization phases and stages

According to the cross-cutting relationships of the ore veins, mineral assemblages, paragenetic sequence and ore fabrics, the ore-forming process can be divided into two mineralization phases: hydrothermal phase and supergene phase. The hydrothermal phase can be further divided into four mineralization stages; they are (from early to late) stages I, II, III and IV.

Stage I is the pyrite-quartz stage, characterized by the occurrence of large quartz veins, 0.5–5.0 m thick, along the high-angle fault. The mineral assemblage is simple, dominated by quartz with minor spotted pyrite, and ankerite can be seen in local places. Gold mineralization is poor and the content of gold is commonly <1 g/t.

Stage II represents a barite stage, characterized by the presence of pure barite veins, distributed in the middle of quartz-barite compound veins or forming single barite veins (e.g. No. I vein). The principal mineral is barite, with minor pyrite and siderite. The barite formed in this stage is white and coarse in grain size, and most of them are euhedral crystals. Gold began to be precipitated in this stage.

Table 1 Features of ore veins and gold orebodies in the Bulong gold deposit

Ore vein number	Quartz-barite vein			Gold orebody			
	Length (m)	Thickness (m)	Occurrence	Length (m)	Width (m)	Thickness (m)	Average Au grade (g/t)
I (barite vein)	125	2.3	85°–110°∠50°–60°				0.45
II	230–660	0.50–1.0	320°–10°∠10°–28°	85–450	240	0.34	3.72
III	400–630	0.80	320°–10°∠10°–25°	280–400	360	0.50	2.74
IV	310	1.0	320°–0°∠10°–25°	81		0.42	1.64
VII	15	0.50	42°∠20°	15		0.50	5.66

Note: after No. 8 Geological Party, Xinjiang Bureau of Geology and Mineral Exploration and Development, 1999.

Stage III is the pyrite-siderite-barite-quartz stage, mainly characterized by the formation of quartz veins, barite-quartz veins and calcite-barite-quartz veins, ranging in thickness from several centimeters to 50 cm. The veins are distributed in the upper, lower and marginal parts of the ore veins or form single ore veins (e.g. No. VII), and the quartz veins is slightly earlier than the other veins. Calcite-barite-quartz veins mostly occur as lenses or patches. In the contact zone between the quartz veins or barite-quartz veins and pure barite veins, the veinlets of the former can be seen to penetrate into the latter on the outcrop, and the quartz veinlets or stockworks may also be observed to be distributed in pure barite veins under the microscope. The mineral assemblage includes calcite, siderite, ankerite, pyrite and native gold. Barite is mostly anhedral granular, 0.2–0.4 mm in grain size, in mosaic contact with quartz. This stage was the main stage of gold mineralization in the Bulong deposit, when gold was precipitated in large amount.

The ore types of stage III are simple, being mainly of auriferous quartz-barite vein and auriferous quartz vein types and in a few cases of auriferous breccia type (e.g. No. VII ore vein). Ores mainly have euhedral, subhedral and anhedral granular textures, metasomatic texture and skeletal texture and disseminated, veinlet-stockwork, vein, massive and brecciated structures. The brecciated structure only occurs in No. VII orebody, with siltstone and barite clasts and quartz cement. The visible gold grains are distributed either at the contacts between quartz and clasts or in honeycomb pores resulting from weathering of sulphides.

Metallic minerals in ores account for less than 1%, and the dominant ones are pyrite, siderite, limonite and native gold, with minor chalcopyrite, bornite and malachite. Nonmetallic minerals are mainly barite and quartz; calcite and ankerite are less abundant and sericite, chlorite, and feldspar just occur locally.

Stage IV is the carbonate stage, in which mainly calcite veinlets or ankerite veinlets formed. The veinlets are several millimeters to 20 mm wide and spread mainly along the fractures in the wall rocks, and a few penetrate into ore veins. This stage hints the end of the ore-forming processes, and the gold content of the ores is lower.

3.3 Wall rock alteration

Wall rock alteration is rather strong, especially in wall rocks of Nos. II, III, IV and VII ore veins, where linear alteration along the faults is well developed. Wall rock alteration types include silicification, pyritization, sideritization, sericitization, chloritization, calcitization, ankeritization and limonitization, of which the silicification, pyritization, sideritization and ankeritization are closely associated with the gold mineralization. Silicification is well developed in the deposit, which can be divided into two phases at least. In the first phase siltstone recrystallized into quartz aggregates, forming secondary quartzite 1–2 mm thick in local wall rocks of orebodies. In second phase silicification resulted in the formation of quartz veinlets and calcite-quartz veinlets, 1–5 mm thick, which are distributed unevenly. Pyritization mainly occurs in wall rocks close to orebodies, and the closer to the contact zone of the orebodies and wall rocks, the higher the pyrite content, the larger the grain size and higher the degree of idiomorphism of the pyrite. Small amount of pyrite occurs as disseminations in the auriferous (barite) quartz veins, and pyrite can be seen occasionally in the large quartz veins. Pyrite in the ore veins is fine-grained ($\leqslant$ 0.5 mm in diameter), but it is coarser in the wall rocks, generally 0.5–1.0 mm in size, and the coarsest ones can reach 4–8 mm. Pyrite occurs as pentagonal dodecahedrons and cubes and partially as subhedral-anhedral grains; they assume the form of glomerocrysts or single crystals. Most of pyrite has been limonitized. Sericitization is best developed in the wall rocks close to orebodies, which shows a fine flaky texture.

3.4 Modes of occurrence of gold and characteristics of the gold mineral

Gold occurs in the form of native gold and has three modes of occurrence: (1) intergranular gold between quartz grains or between quartz grains and barite grains, (2) fissure gold distributed in fissures of pyrite (limonitized), and (3) gold mineral hosted in quartz grains or barite grains.

Native gold is gold-yellow in colour, with strong metallic luster, and mainly occurs as grains, irregular dendritic aggregates and sheets and occasionally as incomplete cubic crystals. The grain size varies greatly from particles to huge grains. The grain size of fissure gold in pyrite pseudomorphs is < 0.01 mm, while visible gold is generally 0.1–3 mm and the largest one may be up to 5 mm. Visible gold occurs mainly as secondary gold in honeycomb-shaped pores and subordinately as primary gold. Microprobe analysis gave the following composition (%) of native gold: Au 97.85, Ag 0.60, Cu 0.13, Zn 0.13, Cd 0.09, Sb 0.18, Fe 0.05, Co 0.08, Te 0.05, Mo 0.02, S 0.02 and Ni 0.22 (No. 8 Geological Party of the Xinjiang Bureau of Geology and Mineral Exploration and Development, 1994). The content of silver in the gold mineral is low and the fineness of gold is as high as 994.

4 Sulphur Isotopic Composition

Ten fresh pyrite samples (five from the pyrite-quartz stage) and ten barite samples (from the barite stage) were

selected under the binocular microscope, and their purities were over 99%. The sulphur isotopic composition was analyzed at the Stable Isotope Laboratory, Institute of Mineral Resources, Chinese Academy of Geological Sciences. Cu_2O was used as the oxidizer for the preparation of sulphide samples. Sulphate minerals were purified to pure $BaSO_4$ by the carbonate-zinc oxide semi-melt method, and then SO_2 was prepared by the V_2O_5 oxide method. The SO_2 released was measured for sulphur isotopes at a MAT 251 mass spectrometer, using VCDT as the standard material. The analytical precision was ±0.2%. The $\delta^{34}S$ values of pyrite range from 14.6 to 19.2‰ with a mean of 17.6‰, while those of pyrite from wall rocks near the gold vein range from 14.6 to 17.67‰ with a mean of 16.46 ‰, and those of pyrite from the large auriferous quartz vein are slightly higher, ranging from 18.5 to 19.2 ‰ with a mean of 18.94 ‰. The $\delta^{34}S$ values of barite range from 35.0 to 39.6 ‰ with a mean of 37.3‰ (Table 2; Fig. 3).

Table 2 Sulfur isotopic composition of the Bulong gold deposit

Ser. No.	Sample	Mineral	$\delta^{34}S_{VCDT}$ (‰)	Ser. No.	Sample	Mineral	$\delta^{34}S_{VCDT}$ (‰)
1	BL-3-13	Pyrite	16.6	11	BL-2-2	Barite	37.5
2	BL-3-14	Pyrite	16.8	12	BL-2-6	Barite	37.8
3	BL-3-15	Pyrite	14.6	13	BL-3-4	Barite	38.8
4	BL-3-16	Pyrite	16.0	14	BL-3-6	Barite	35.8
5	BL-3-18	Pyrite	17.1	15	BL-3-7	Barite	35.0
6	BL-8-1	Pyrite	19.1	16	BL-3-19	Barite	39.6
7	BL-8-2	Pyrite	19.2	17	BL-3-24	Barite	35.4
8	BL-8-3	Pyrite	19.2	18	BL-3-43	Barite	39.1
9	BL-8-4	Pyrite	18.7	19	BL-4-5	Barite	36.8
10	BL-8-5	Pyrite	18.5	20	BL-4-6-1	Barite	37.2
11		Pyrite	17.67	21		Barite	36.75

Note: Serial No. 11 and 21 are after Zheng et al., 1996: 1–5 from the pyritized wall rock near the gold lode and 6–10 from the auriferous large quartz vein. Analyzed by Luo Xurong and Bai Ruimei.

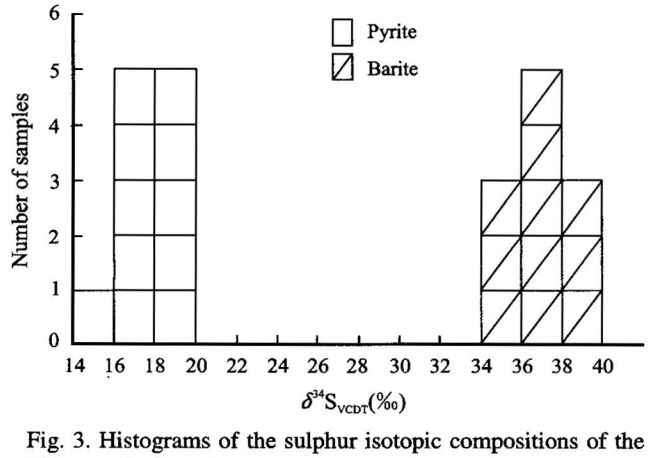

Fig. 3. Histograms of the sulphur isotopic compositions of the Bulong gold deposit.

5 Helium and Argon Isotope Compositions of Metallogenic Fluids

As a new effective method, the inert gas isotope analysis has been widely applied to studying the Earth's evolution, mantle degassing, tectonic settings, fluid migration, source of ore materials and so on (Wang and Mao, 1996; Wang Denghong et al., 2002; Niu et al., 2003). The marked difference in isotopic compositions of inert gases in crustal and mantle materials may serve as an important indication for tracing the source of ore-forming fluids. In this study, the helium and argon isotope system was used to trace the source of ore-forming fluids of the Bulong gold deposit.

5.1 Samples and analytic methods

Ten samples were selected for helium and argon isotope measurements, of which five were collected from the pyritized wall rocks near orebodies and five from the pyrite-quartz stage of the large auriferous quartz vein. Pyrite is known to be an ideal trap for inert gases, whose leaking degree is much lower than those of other minerals. The influences of the isotope fractionation and epigenetic process caused by diffuse He and Ar loss from fluid inclusions on the He and Ar isotopic compositions may be negligible (Hu et al., 1999). Each pyrite sample was picked using a binocular microscope and its purity was over 99%. Helium and argon isotopes were analyzed at the Stable Isotope Laboratory, Institute of Mineral Resources, Chinese Academy of Geological Sciences. The analytical procedure is as follows (Mao et al., 1997, 2002; Li et al., 2000, 2001): Each sample weighed ~ 1–2 g, which was cleaned by acetone in an ultrasonic bath and then dried in an oven. Samples were loaded into screw-type crushers and baked on-line at 100–150°C for 24 hours to remove absorbed atmospheric gases before crushing. Gases were extracted from the fluid inclusions by manual crushing in vacuum. The released gases were purified four times by the titanium sponge getter, zircon-aluminum getter, active carbon and liquid nitrogen cooling trap, and the active gases such as H_2, N_2, O_2, CO_2, CH_4 and H_2O and organic substances were all frozen and absorbed. The remaining gases were exposed in a zircon-aluminum pump to be frozen for ten minutes, and Ar and Xe were then condensed onto liquid N_2-cooled charcoal. Comparatively pure He and Ne were sent into the analysis system. Trace impure gases such as H_2 and Ar entering into the analysis system together with He and Ne were re-purified and removed by a liquid N_2-cooled titanium sublimation pump. The helium isotopic composition was measured on a MI-1201 IG inert gas mass spectrometer made in Ukraine. ^4He was received by a Faraday cup and ^3He by an electron multiplier. The

amplification coefficient of the electronic multiplier was 1×10^5 and its resolution was 1200, so that the peaks of ^3He and $HD+H_3$ can be completely separated from each other, needless to correct $HD+H_3$. Ar was desorbed on the charcoal finger and separated from Xe at –78°C. ^{40}Ar was received by a Faraday cup and ^{36}Ar and ^{38}Ar by an electronic multiplier. The standard gas for work was measured before analyzing the samples, and the measurement results of samples were normalized to the standard gas, which was made by purifying the air and periodically examined by the air during measurements. All the analytical results are based on the international atmosphere standard, whose $^3He/^4He$ ratio is 1.40×10^{-6}. All the results of helium were given in the $^3He/^4He$ ratio and R/Ra ratio, where R is the $^3He/^4He$ ratio of the sample and Ra is that of the air. The blank level of ^4He was 2×10^{-11} cm^3 STP, the blanking $^3He/^4He$ ratio was 1×10^{-6} and the blank level of ^{40}Ar was 5×10^{-9} cm^3. The effect of the blank on the measurement result was negligible. The analytical precision of the standard gas was 1% and those of samples are shown in Table 3.

5.2 Analytical results of helium and argon isotopes

The helium and argon isotopic compositions of fluid inclusions in pyrite from the Bulong gold deposit are shown in Table 3. The $^3He/^4He$ ratios of fluid inclusions in pyrite are 0.24–0.82 R/Ra, $^{40}Ar/^{36}Ar$ ratios are 338–471 and $^{40}Ar/^4He$ ratios are 0.015–0.412. The data show that the isotope compositions of pyrite in the wall rocks near orebodies are somewhat different from those of the large quartz veins. For the former, the R/Ra ratios of fluid inclusions are 0.24–0.66 with a mean of 0.49, $^{40}Ar/^{36}Ar$ ratios are 338–376, and $^{40}Ar/^4He$ ratios are 0.015–0.118, except for sample BL-3-16 whose $^{40}Ar/^4He$ ratio is 0.412. For the latter, those ratios are slightly higher: the R/Ra ratios are 0.55–0.82 with a mean of 0.71, $^{40}Ar/^{36}Ar$ ratios are 395–471 and $^{40}Ar/^4He$ ratios are 0.117–0.222. The data are consistent with the marked differences in the geological characteristics, gold content and ore-forming stages of both quartz-barite veins and large quartz veins.

6 Discussion

6.1 Source of ore-forming materials

The sulphur isotopic compositions of pyrite and barite are homogeneous and the $\delta^{34}S$ values have a narrow range, which shows the sulphur in ore-forming fluids was derived from a single source. The appearance of barite or the barite + pyrite assemblage suggests that the deposit formed at a high oxygen fugacity, implying that the $\delta^{34}S$ value of barite is equivalent to or slightly higher than the total $\delta^{34}S$ values of the hydrothermal fluids (Zheng and Chen, 2000), i.e. in the Bulong gold deposit the total $\delta^{34}S$ values of the hydrothermal fluids range from 35.0‰ to 40.0‰. The $\delta^{34}S$ values of the pyrite are similar to those (9‰–32‰) of marine sulphate (Zheng and Chen, 2000), but the total $\delta^{34}S$ values of the hydrothermal fluids are notably higher than these values, indicating that the sulphur came from the strata and was related to reduction of sulphate.

The sulphur isotope composition of the Bulong gold deposit is apparently distinct from those of VMS type deposits, Carlin-type gold deposits, low-sulphur or high-sulphur epithermal gold deposits and medium- and low-temperature hydrothermal gold deposits (Table 4). The $\delta^{34}S$ values of Bulong gold deposit are all positive and characterized by enrichment of heavy sulphur. The $\delta^{34}S$ values of barite are as high as 35.0‰–39.6‰ with a mean of 37.3 ‰, which is rather rare in hydrothermal deposits but similar to that of barite from SEDEX barite deposits. For example, the $\delta^{34}S$ values of the Xinhuang Gongxi-Tianzhu Dahebian barite deposit located on the border between Hunan province and Guizhou province may reach 32.34‰–

Table 3 Helium and argon isotopic compositions of fluid inclusions in pyrite from the Bulong gold deposit

Ser. No.	Sample	Mineral	$^3He/^4He$ ($\times10^{-7}$)	^4He ($\times10^{-6}cm^3/g)_{STP}$	R/Ra	$^{40}Ar/^{36}Ar$	$^{40}Ar/^{38}Ar$	$^{36}Ar/^{38}Ar$	^{40}Ar ($\times10^{-7}cm^3/g)_{STP}$	$^{40}Ar/^4He$	He_{mantle} (%)
1	BL-3-13	Pyrite	3.32±0.53	8.02	0.24	376±4	2068±10	5.52±0.04	6.85	0.085	2.84
2	BL-3-14	Pyrite	8.38±1.26	2.16	0.60	351±3	1913±24	5.28±0.06	2.54	0.118	7.45
3	BL-3-15	Pyrite	5.41±0.96	10.78	0.39	338±3	1878±13	5.56±0.05	4.13	0.038	4.74
4	BL-3-16	Pyrite	9.28±1.91	1.24	0.66	356±6	1978±47	5.53±0.23	5.11	0.412	8.27
5	BL-3-18	Pyrite	7.79±1.78	0.99	0.56	369±6	2025±25	5.37±0.20	0.15	0.015	6.91
6	BL-8-1	Pyrite	11.47±2.14	4.56	0.82	429±3	2296±25	5.32±0.16	8.20	0.18	10.26
7	BL-8-2	Pyrite	11.04±1.00	2.68	0.79	395±6	2186±28	5.53±0.03	3.14	0.117	9.87
8	BL-8-3	Pyrite	10.24±2.82	3.58	0.73	427±34	2349±112	5.56±0.41	5.27	0.147	9.14
9	BL-8-4	Pyrite	7.70±1.10	3.94	0.55	463±9	2504±40	5.38±0.02	8.7€	0.222	6.83
10	BL-8-5	Pyrite	8.90±0.67	3.25	0.64	471±9	2533±17	5.34±0.10	6.21	0.191	7.92

Note: Analyzed by Song Hebin and Li Yanhe.

Table 4 Comparative features of different types of gold deposits

Type	Deposit	Host rocks	Occurrence relations between orebody and wall rock	Wall-rock alteration	Main mineral assemblages	Gold ore type	Occurrence of barite	$\delta^{34}S$(‰) of pyrite	$\delta^{34}S$(‰) of barite	Source of sulfur	References
Quartz-barite vein type	Bulong Au deposit	Fine clastic rock	Generally concordant, locally cutting bedding	Silicification, pyritization, carbonation, sericitization etc.	Quartz, barite,native gold, minor pyrite and carbonate etc.	Quartz-barite vein and quartz vein	Vein	14.6 – 19.2	35.0 – 39.6	Strata, associated with reduction of sulfate	This paper
Sedex	Barite deposit in Xinhuang, Gongxi–Tianzhu, Dahebian	Siliceous rock and carbonaceous shale with phosphorite	Concordant		Barite(98%), calcite, pyrite, sericite, muscovite, organic matter etc.		Stratified, local lenticular	14.6 – 24.2	32.34 – 41.56	Sea water, associated with organic matter and biological activities	Wang et al., 1991; Che , 1995; Wu et al., 1999
	Jingtieshan Fe deposit, Gansu province	Phyllite, quartzite	Concordant		Specularite, siderite, pyrite, chalcopyrite, barite, carbonate etc.		Stratified, banded and lenticular	8.1 – 15.6	19.7 – 33.6	Sulfate from sea water	Mao et al., 2003
VMS	Ashele Cu-Zn deposit, Xinjiang	Spilite–quartz keratophyre and tuff	Concordant	Silicification, sericitization, chloritization, pyritization, epidotization and alunitization etc.	Pyrite, chalcopyrite, sphalerite, tetrahedrite, barite, quartz etc.		Stratified and banded	1.3 – 8.17	16.4 – 20.3	Multiple sources including volcanic exhalation, sulfate from sea water etc.	Wang, 1996; Jia, 1996; Ye et al., 1997;
	Gacun Au-Cu polymetallic deposit, Sichuan Province	Mafic volcanic rock, felsic volcanic rock	Concordant	Silicification, sericitization, chloritization, epidotization, kaolinite, calcitization etc.	Pyrite, sphalerite, galena, chalcopyrite, barite, quartz, jasper etc.		Stratified and banded	– 4.6 –3.1	13.8 – 22.5	Volcanic activity and seawater	Yu et al., 2000; Chen et al., 2001; Hou et al., 2001
Carlin-type gold deposit	Laerma Au deposit, Gansu province	Carbonaceous sericite slate , carbonaceous siliceous slate	Generally concordant	Silicification, sericitization, stibnitization, barite, dickite, carbonation	Native gold, pyrite, stibnite, chalcopyrite, cinnabar, quartz, barite dickite etc.	Siliceous rock type , slate type and dacite porphyry type	Disseminated (gold-bearing), vein (late mineralization stage)	–32.25 – –25.20 1.62 – 21.48	2.41 – 28.5	Sedimentary sulfur in siliceous formation	Yao , 1994; lin et al., 1998; Liu et al., 2000; Mao et al., 2002b
	Banqi Au deposit, Guizhou province	Siltstone, fine siltstone, claystone	Generally concordant; orebody occurs in footwall of fault	Silicification, argillation, carbonation, pyritization, baritization, arsenopyritization etc.	Pyrite, arsenopyrite, marcasite, stibnite, chalcopyrite, dickite, barite etc.	Siliceous ore, silty ore, pyrite ore, arsenopyrite ore	Forming veinlet with calcite, occurring in late mineralization stage	6.72 –14.7		Strata and mantle	Liu et al., 1999; Ying, 2001; Gao et al., 2002; Hu et al., 2002
	Carlin-type Au deposit in America	Marine carbonate rock and fine clastic rock	Discordant	Silicification-jasperoidization, pyritization, carbonation, arsenopyritization, baritization, realgar, arsenopyritization, orpiment etc.	Pyrite, orpiment, realgar, stibnite, cinnabar, chalcopyrite, native gold, kaolinite, barite, plaster, clay mineral etc.	Normal type, siliceous type, pyrite type, carbonaceous type and arsenic-rich type	Vein, formed in late mineralization stage	–7 – 17	15 – 25	Sulfate	Gao et al., 2002; Radtke, 1980; Hu et al., 2002; Cline and Hofstra, 2000; Emsbo et al., 1999; Arehart, 1996
Medium-low temperature hydrothemal gold deposit	Dongfengding Au deposit, Shangxi province	carbonate rock, clastic rock	Discordant	Silicification, limonitization, baritization	Quartz, pyrite, limonite, barite etc.	Quartz gold ore, limonite quartz gold ore, limonite gold ore, gold-bearing (poor gold potential) barite ore	Vein, formed in late mineralization stage	1.9 – 5.7 rarely 29.4	4.7	Metamorphic rock of basement	He et al, 1995
Low-sulfide epithermal gold deposit	Axi Au deposit, Xinjiang	Pyroclastic rock, lava	Discordant	Sericitization, adularization, silicification, chloritization, propylitization, argillation etc.	Pyrite, marcasite, arsenopyrite, sphalerite, adularia, quartz, few barite	Quartz vein, altered rock, breccia	Disseminated	0.95–10.15		Deep or magma source	Chen et al., 2001; Bao et al., 2002
High-sulfide epithermal gold deposit	Zijinshan Cu-Au deposit, Fujian province	Dacitic porphyrite, breccia	Discordant	Silicification, dickite, alunitization, sericitization and pyritization	Pyrite, native gold, chalcopyrite, digenite, quartz, dickite, barite	Oxidized ore	Veilet filling in fracture	– 8.4 –6.9		Mantle source	Xu et al., 1997; Zhang et al., 1999

41.65‰ (Wu et al., 1999; Che, 1995; Wang and Li, 1991), the $\delta^{34}S$ values of the Liuling barite deposit in the Qinling region are 31.8‰–40.1‰ (Wang and Li, 1991), the $\delta^{34}S$ values of the Jingtieshan iron deposit in Gansu province are 19.7‰–33.6‰ with a mean of 29.1‰ (Mao et al., 2003), the $\delta^{34}S$ values of the Vulcan barite deposit in Canada is 43.5‰ (Mako and Shanks, 1984). Many researchers (Wu et al., 1999; Che, 1995; Wang and Li, 1991; Maynard and Okita, 1991) suggested that the sulphur in barite originates from marine sulphate, and that organic materials, bacteria and biological activities can cause intense fractionation of sulphate ions, thus making $\delta^{34}S$ become more concentrated. The Bulong gold deposit belongs to the hydrothermal vein deposit and its age is distinctly younger than that of its host strata; since no marine environment was in existence, organic materials or bacteria were impossible to cause reduction of sulphate in sea water. Therefore, the sulphide in the Bulong deposit is likely to be the product of inorganic reduction of marine sulphate. In addition, the $\delta^{34}S$ values of barite are higher than those of its contemporary sulphate in sea water, suggesting that it went through fractionation caused probably by the hydrothermal activity.

6.2 Source of ore fluids

The $^3He/^4He$ ratios of fluid inclusions in pyrite are 0.24–0.82 R/Ra, which are ten times higher than that of the crust (0.01–0.05 R/Ra) (Stuart et al., 1995) but 10–30 times lower than that of the mantle (6–9 R/Ra). On the diagram of ^3He versus ^4He (Fig. 4), all of the data points of the helium isotope composition of fluid inclusions in pyrite plot between the crustal end-member and the mantle end-member, near the side of the crustal. The percentage of mantle-derived He can be calculated according to the crust-mantle mixing model, which is expressed as:

$$He_{mantle}(\%) = \{(^3He/^4He)_{sample} - (^3He/^4He)_{crust}\}/\{(^3He/^4He)_{mantle} - (^3He/^4He)_{crust}\}\times 100$$ (Xu et al., 1996, 1998).

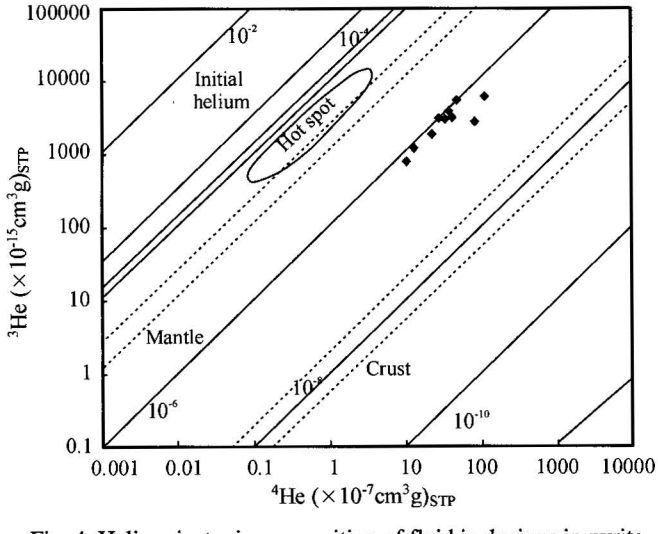

Fig. 4. Helium isotopic composition of fluid inclusions in pyrite from the Bulong gold deposit (modified from Mamyrin and Tolstikhin, 1984).

where the lower limit of $^3He/^4He$ of the crust end-member is 2×10^{-8} and that of the mantle is 1.1×10^{-5} (Stuart et al., 1995). The calculation results show that the percentage of the mantle-derived He in the pyrite ranges from 2.84 to 10.26 (Table 3), averaging 7.42. In general, the $^3He/^4He$ ratios of ore fluids in the Bulong gold deposit are close to the crustal characteristic value, reflecting that the ore fluids mainly came from the crust and were mixed with a small amount of the mantle component in the metallogenic process. The helium isotope features of ore fluids in the Bulong gold deposit obviously differ from those of some hydrothermal deposits in China, such as the Dashuigou tellurium deposit, Wangu gold deposit, Machangqing copper deposit, Ailaoshan metallogenic belt, Jiaodong gold deposits and Dongping gold deposit, which are reported to have involved some mantle-derived fluids during mineralization. The R/Ra values of ore-forming fluids in those deposits are 0.1–3.0 (Hu et al., 1997, 1999; Mao et al., 1997; Mao and Wei, 2000; Zhang Lianchang et al., 2002; Deng et al., 2003) and the R/Ra values for the Dongping gold deposit are higher, ranging from 0.3 to 5.2 (Mao and Li, 2001); whereas the R/Ra values of ore-forming fluids of the Wangu gold deposit may reach up 3.5–9.8, showing that the dominant ore-forming fluids were derived from the mantle (Mao et al., 2002a).

The $^{40}Ar/^{36}Ar$ ratios of ore-forming fluids in pyrite are 338–471, which are slightly higher than that of the atmosphere ($^{40}Ar/^{36}Ar$=295.5), indicating the existence of small amount of excess argon produced probably by higher radiogenic ^{40}Ar. The $^{40}Ar/^4He$ ratios of mantle fluids are 0.33–0.56 (Dunai and Touret, 1995) and the average value of the crust is ~ 0.2 (Stuart et al., 1995; Hu et al., 1997). The $^{40}Ar/^4He$ ratios of ore fluids in the Bulong gold deposit are 0.015–0.222 with a mean of 0.153, except for one sample which gives 0.412; these ratios are similar to the value of the crust. The diagram of $^3He/^4He$ (R/Ra) vs. $^{40}Ar/^{36}Ar$ of fluids in pyrite from the Bulong deposit (Fig. 5) shows that the data points of the Bulong gold deposit are close to the field of the crustal fluid component, indicating that the ore fluids were mainly derived from the crust.

6.3 Comparative study

Barite deposits are mainly of the sedimentary and hydrothermal type. The main characteristics of SEDEX-type barite deposits are as follows: orebodies occur in sedimentary rocks, most of which are black rock series; the orebodies are stratified, concordant with the bedding of host strata; the ores have banded and laminated structures,

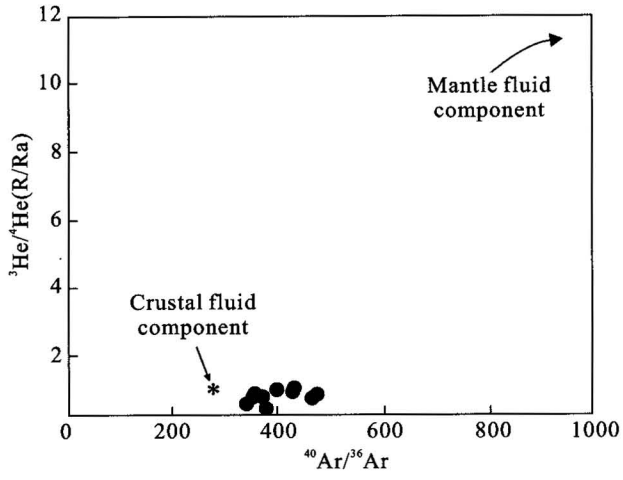

Fig. 5. Plot of $^{3}He/^{4}He$ (R/Ra) vs. $^{40}Ar/^{36}Ar$ ratios of the fluids in pyrite from the Bulong gold deposit (modified from Mao et al., 2002).

showing typical sedimentary features. Barite is the important component in some SEDEX-type lead-zinc deposits, such as the Tom deposit, Sivermines deposit and Meggen deposit. The barite in the Jingtieshan SEDEX-type iron deposit is so rich to reach a large barite deposit. Barite in the above-mentioned deposits is stratified and massive-stratified, alternating with or occurring inside or around sulphide (or specularite), and there exist jasper interbeds between barite beds and layered sulphide (Mao et al., 2003). In massive sulphide deposits (VMS) hosted in marine volcanic rocks, barite is generally well developed, which occurs in the stratified and massive forms, alternating with massive sulphide, and ores show banded or laminated structure. Mineralization zonation is distinct in VMS deposits, such as Kuroko deposits (Urabe and Sato, 1978) and black chimney-type deposits in the Okinawa Trough back-arc basin, Japan (Halbach et al., 1989), the Gacun deposit in Sichuan (Hou et al., 2001) and the Ashele deposit in Xinjiang (Liu and Zhou, 1999; Jia, 1996). Barite from the Bulong deposit has entirely different characteristics from the above-mentioned deposits (Fig. 4), and both quartz-barite compound veins and barite veins show no sedimentary features or zonation but the characteristics of epigenetic-hydrothermal vein-type deposits.

Carlin-type gold deposits are a kind of finely disseminated, medium- and low-temperature hydrothermal gold deposit, also called fine disseminated gold deposits, which are hosted in fine clastic rocks, carbonate rocks and siliceous rocks that have not undergone regional metamorphism. An assemblage of middle- and low-temperature, hydrothermal sulphide and alteration minerals is developed in such deposits. They form mainly at medium temperatures (Kuehn and Arthur, 1995) and gold grains are submicroscopic-microscopic (Romberger, 1986; Zhang Fuxin et al., 1998). Barite is pervasive in Carlin-type gold deposits and mostly occurs as veinlets or veins. It forms in the late mineralization stage (Ying, 2001) and is not closely related to gold mineralization, as exemplified by the Carlin and Alligator Mountains gold deposits in the United States (Radtke et al., 1980; Gao et al., 2002), Shangmanggang and Banqijin gold deposits in Yunnan province and the La'erma gold deposit in Gansu province. In the Bulong gold deposit, host rocks are fine clastic rocks, orebodies are barite-quartz veins, sulphide in ore is rare, the alteration mineral assemblage characteristic of Carlin-type gold deposits is lacking, the gold is closely associated with quartz and barite, the majority of gold occurs as micrograins, and visible gold is well developed. All these features indicate that the Bulong deposit does not belong to the Carlin-type gold deposit.

Epithermal gold deposits are mainly hosted in continental igneous rocks (Ying, 1999), which are closely related to porphyry deposits (Heald et al., 1987; love et al., 1998; Zhang Dequan et al., 2003), and their two end-members are low-sulphurization epithermal and high-sulphurization epithermal gold deposits. Low-sulphurization epithermal gold deposits are characterized by the presence of large amounts of adularia and sericite, which are controlled by either calderas or composite faults—fracture system—far away from the calderas and often associated with regional Hg-Sb and Pb-Zn deposits (Jiang and Wang, 2002). High-sulphurization epithermal gold deposits are characterized by formation of substantial amount of alunite, kaolinite and other advanced argillic alteration (Berger and Henley, 1998) and closely associated with volcanic edifices in space. In the low- or high-sulphurization epithermal gold deposits, there also occurs a small amount of disseminated or veinlet barite, which has no necessary relation with gold mineralization, as exemplified by the Axi gold deposit in Xinjiang (Chen et al., 2001; Bao et al., 2002; Jiang and Wang, 2002), Yelmend gold deposit in Xinjiang (Xiao et al., 2001) and the Zijinshan copper-gold deposit in Fujian (Zhang Dequan et al., 1991, 2003; Xu et al., 1997). In the Bulong gold deposit and its surroundings, volcanic rocks and porphyry are not seen, and the main alteration indications for the epithermal metallogenic system such as alunite, kaolinite and K-feldspar are not recognized in altered wall rocks either.

To sum up, the Bulong gold deposit, as a special type of deposit, is a rare quartz-barite vein type gold deposit in China.

6.4 Genesis of the deposit

The homogenization temperatures of fluid inclusions in

barite and quartz from ores are 159–390°C, mineralization pressures are 140×10^5–200×10^5 Pa, and mineralization depths are 500–800 m (Yang et al., 1999), which show the characters of hypabyssal, medium-temperature metallogenesis.

The Bulong gold deposit is located near the regional Karateki fault, where well-developed secondary faults serve as pathways and spaces for migration and accumulation of hydrothermal solution. Gold contents of the Upper Devonian clastic rocks and Upper Carboniferous carbonate rocks in the ore district or its surroundings are several to tens of times higher than the regional background values, indicating that the strata provided ore materials for gold mineralization. Two hidden plutons occur in the northeast and southeast of the area (Wang Weiping, 2001), which provided energy for convective circulation of fluids. Therefore, the ore-forming processes of the Bulong gold deposit can be described as follows: The interlayer water stored in wall rock formation and meteoric water infiltrating down along the faults was heated at depth, forming the initial hydrothermal ore solutions, which activated and extracted ore-forming materials such as gold and sulphur from the strata and mixed with a small quantity of mantle fluids to form hydrothermal ore solutions. Driven by magmatic heat, hydrothermal ore solutions circulated and migrated upward along faults, and when the hydrothermal ore solutions migrated to the near-surface interlayer fracture zones and faults, with the decrease in pressure and rapid change in physicochemical conditions and in the oxidizing environment, ore materials were precipitated from the ore solutions to form the quartz-barite vein type gold deposit.

7 Conclusions

(1) Host rocks of the Bulong gold deposit are Late Devonian phyllitized and schistose fine clastic rocks, which have the features of flyschoid formations. Occurring at the intersections of the regional Karateki fault and its subsidiary faults, the deposit is strongly controlled by fault structures and the gold orebodies are hosted by interlayer and gently inclined fracture zones, while auriferous large quartz veins are controlled by a group of steeply inclined faults.

(2) Barite veins, big quartz veins and quartz-barite veins occur in the ore district. For the first two kinds of veins, there appears only gold mineralization. Gold orebodies occur in quartz veins and barite-quartz veins of the upper and lower parts of the quartz-barite compound veins. The orebodies are bedded in shape and the average gold grade of the ores ranges from 1.64–3.72 g/t. The types of wall rock alteration mainly include silicification, pyritization, carbonatization and sericitization. Ore types are simple, and there is rare sulphide in the ore, only minor pyrite being present. The Bulong gold deposit is of the quartz-barite vein type, a rare gold type in China.

(3) The $\delta^{34}S$ values of the pyrite range from 14.6‰ to 19.2‰ with a mean of 17.6‰ and those of barite from 35.0‰ to 39.6‰ with a mean of 37.3‰. The $\delta^{34}S$ values of the barite is equal to or slightly higher than the total $\delta^{34}S$ values of the hydrothermal fluids, which indicates that the sulphur came from the strata and was related to the reduction of sulphate.

(4) The $^3He/^4He$ ratios of fluid inclusions in the pyrite are 0.24–0.82 R/Ra, close to that of the crust, which indicates that the ore-forming fluids came from the crust. The $^{40}Ar/^{36}Ar$ ratios are 338–471, slightly higher than that of the atmosphere. The $^{40}Ar/^4He$ ratios of the ore-forming fluids are 0.015–0.412 with a mean of 0.153, which are similar to the value of the crust. The helium and argon isotopic compositions of fluid inclusions show that the ore-forming fluids were mainly derived from the crust.

Acknowledgments

We are grateful to the No. 8 Geological Party of the Xinjiang Bureau of Geology and Mineral Exploration and Development, the Akqi Administration of Mineral Resource and the Bulong Gold Mine for their supports and helps. Mr. Amantuer is thanked for his help during the fieldwork. Thanks are also due to Li Yanhe, Song Hebin, Luo Xurong and Bai Ruimei for their assistance in the isotope analysis. This work was financially supported by the Ministry of Science and Technology of China (grants G 2001CB 409807, G 1999043216).

Manuscript received Dec. 26, 2003
accepted Feb. 20, 2004
edited by Liu Xinzhu

References

Arehart, G.B., 1996. Characteristics and origin of sediment-hosted disseminated gold deposits: a review. *Ore Geol. Rev.*, 16: 383–403.

Bao Jingxin, Chen Yanjing, Zhang Zengjie, Chen Huayong and Liu Yulin, 2002. The preliminary study of laumontitization of Axi gold deposit and paleogeothermal minerogenetic fluid system in West Tianshan. *Acta Sci. Natur. Universitatis Pekinensis*, 38(2): 252–259 (in Chinese with English abstract).

Berger, B.R., and Henley, R.W., 1998. Advances in the understanding of epithermal gold-silver deposits, with special reference to the Western United State. *Econ. Geol.*, 6: 405–423.

Che Qinjian, 1995. A metallogenic model for sedimentary Gongxi-type barite deposits. *Geotectonica et Metallogenia*, 19 (3): 288–289 (in Chinese).

Chen Yuchuan, Li Zhaonai, Mu Ruishen, Shen Baofei, Zou Guanghua, Li Huaqin, Wang Quanming, Lin Wemwei, Li Wenkang, Liu Gouqun, Ou Yangzongqi, Meng Fanyi, Wang Denghong, Zhang Zhaochong, Mao Debao, Chen Fuwen, Li Jingchun and Li Junjian, 2001. *The Gold Deposits and Metallogenic Regularity in China.* Beijing: Geological Publishing House, 111–125 (in Chinese).

Cline, J.S., and Hofstra, A.H., 2000. Ore fluid evolution at the Getchell Carlin-type gold deposit, Nevada, USA. *Eur J. Mineral.*, 12: 195–212.

Dunai, T., and Touret, J.L.R., 1995. Heliun, neon and argon isotope systematics of European lithospheric mantle xenoliths: implications for its geochemical evolution. *Geochim. Cosmochim. Acta*, 59: 2767–2783.

Deng Jun, Yang Liqiang, Sun Zhongshi, Wang Jianping, Wang Qingfei, Xin Hongbo and Li Xinjun, 2003. A metallogenic model of gold deposits of the Jiaodong granite-greenstone Belt. *Acta Geologica Sinica* (English edition), 77(4): 537–546.

Emsbo, P., Hutchinson, R.W, Hofstra, A.H., Volk, J.A., Bettles, K.H., Baschuk, G.J., and Johnson, C.A., 1999. Syngenetic Au on the Carlin trend: implications for Carlin-type deposits. *Geol.*, 27: 59–62.

Gao Zhenming, Li Hongyang, Yang Zhusen, Tao Yan, Luo Taiyi, Liu Xianfan, Xia Yong and Rao Wenbo, 2002. *Metallgenesis and Prospect of the Main Gold Deposit Types in Dianqian Area.* Beijing: Geological Publishing House, 30–101 (in Chinese).

Halbach, P., Nakamura, K., Wahsner, M., Lange, J., Sakai, H., Kaselitz, L., Hanse, R.D., Yamano, M., Post, J., Seifert, R., Michaelis, W., Teichmann, F., kinoshita, M.A., Ishibashi, J., Czerwenski, S., Blum, N., 1989. Probable modern analogue of Kuroko type massive sulfide deposits in the Okinawa Trough back-arc basin. *Nature*, 338: 496–499.

He Wenwu, Lu Jianpei, Sun Jianhe and Ma Xian, 1995. Some metallogenic characteristics of Dongfengding gold deposit and their prospecting significance. *Earth Sci.—J. China Univ. Geosci.*, 20(2): 215–220 (in Chinese with English abstract).

Heald, P., Foley, N.K, and Hayba, D.O., 1987. Comparative anatomy of volcanic-hosted epithermal deposits: Acid-sulfate and adulariasericite types. *Econ. Geol.*, 82(1): 1–26.

Hou Zengqian, Qu Xiaoming, Xu Minggi Fu Deming, Hua Lichen and Yu Jinjie, 2001. The Gacun VHMS deposit in Sichuan Province: from field observation to genetic model. *Mineral Deposits*, 20(1): 44–56 (in Chinese with English abstract).

Hu Ruizhong, Bi Xianwu, Turner, G., and Burnard, P.G., 1997. Helium and argon isotope systematics in pyrite fluid inclusions of Machangqing copper deposit. *Sci. China* (D), 27(6): 503–508 (in Chinese).

Hu Ruizhong, Bi Xianwu, Turner, G., and Burnard, P.G., 1999. Helium and argon isotope of the ore-forming fluids in Ailaoshan metallogenic belt. *Sci. China* (D), 29(4): 321–330 (in Chinese).

Hu Ruizhong, Su Wenchao, Bi Xianwu, Tu Guangchi and Albert, H.H., 2002. Geology and geochemistry of Carlin-type gold deposits in China. *Mineralium Deposita*, 378–392.

Huang Chongke, Bai Ye, Zhu Yusheng, Wang Huizhang and Shang Xiuzhi, 2001. *Copper Deposit of China.* Beijing: Geological Publishing House, 134–142 (in Chinese).

Jia Qunzi, 1996. Geological characteristics and metallogenic environment of the Ashele volcanogenic massive sulfide deposit, Xinjiang. *Mineral Deposits*, 15(3): 267–277 (in Chinese with English abstract).

Jiang Xiaowei and Wang Yongjiang, 2002. Characteristics and genesis of the minerogenetic series of the Axi type gold deposits in the West Tianshan. *Geol. China*, 29(2): 203–207 (in Chinese with English abstract).

Kuehn, C.A., and Arthur, W.R., 1995. Carlin gold deposits, Nevada: Origin in a deep zone of mixing between normally pressured and over-pressured fluids. *Econ. Geol.*, 90: 17–26.

Li Yanhe, Li Jincheng, Song Hebin and liu Xiaochun, 2000. Helium isotope geochemistry of ultrahigh-pressure metamorphic eclogites from the Dabie-Sulu Terrane in east China. *Acta Geologica Sinica* (English Edition), 74(1): 14–18.

Li Yanhe, Li Jincheng, Song Honghebin and Guo Lihe, 2001. Helium isotope of mantle-derived inclusions and high pressure megacrysts from Cenozoic basalt in Eastern China. *Sci. China* (D), 31(8): 641–647 (in Chinese).

Lin Li and Zhu Lidong, 1998. Biomineralization in the La'erma dold deposit of the western Qinling mountains. *Acta Geologica Sinica* (English Edition), 72(1): 65–76.

Liu Jiajun, Zheng Minghua, Liu Jianming and Zhou Dean, 2000. Sulfur isotopic composition and its geological significance of the Cambrian gold deposits in western Qinling,China. *J. Changchun Univ. Sci. Tech.*, 30(2): 150–156 (in Chinese with English abstract).

Liu Xianfan, Ni Shijun, Lu Qiuxia, Jin Jingfu and Zhu Laimin, 1999. Geochemical tracing of ore-forming material sources of Carlin-type gold deposits in the Yunnan-Guangxi triangle area —A case study of the application of the combined silicon isotope geochemistry and siliceous cathodoluminescence analysis. *Acta Geologica Sinica* (English edition), 73(1): 30–39.

Liu Xiaodong and Zhou Taofa, 1999. General geological and geochemical characteristics and ore-forming mechanism of the massive sulfide deposits. *J. Hefei Univ. Tech.*, 22(4): 42–47 (in Chinese with English abstract).

Love, D.A, Clark, A.H, Hodgson, C.J., Mortensen, J.K, Archibald, D.A, and Farrar, E., 1998. The timing of adularia-sericite-type mineralization and alunite-kaolinite-type alteration, Mount Skukum epithermal deposit, Yukon Territoy, Canada: Ar-Ar and U-Pb geochronology. *Econ. Geol.*, 93(4): 437–462.

Mamyrin, B.A, and Tolstikhin, I.N., 1984. *Heliun Isotopes in Nature.* Amsterdam-Oxford-New York-Tokyo: Elsevier, 273.

Mako, D.A, and Shanks, W.C., 1984. Stratiform sulfide and barite-fluorite mineralization of the Vulcan prospect, Northwest Territories: Exhalation of basinal brines along a faulted continental margin: Canadian *J. Earth Sci.*, 21: 78–91.

Mao, J.W., Kerrich, R., Li, H.Y., and Li, Y.H., 2002a. High $^3He/^4He$ ratios in the Wangu gold deposit, Hunan province, China: Implications for mantle fluids along the Tanlu deep fault zone. *Geochem. J.*, 36(3): 197–208.

Mao, J.W., Qiu, Y.Q., Goldfarb, R.J., Zhang, Z., Garwin, S., and Fengshou, R., 2002b. Geology, distribution and classification of gold deposits in the western Qinling belt, central China. *Mineralium Deposita*, 37: 352–377.

Mao Jingwen, Li Yanhe, Li Hongyan, Wang Denghong and Song Hebin, 1997. Helium isotopic evidence on metallgenesis of mantle fluids in the Wangu gold deposit, Hunan Province. *Geol. Rev.*, 43(6): 646–649 (in Chinese with English abstract).

Mao Jingwen and Wei Jiaxiu, 2000. Helium and argon isotopic components of fluid inclusions and tracing to the source of

metallogenic fluids in the Dashuigou tellurium deposit of Sichuan province. *Acta Geosci. Sinica*, 21(1): 58–61 (in Chinese with English abstract).

Mao Jingwen and Li Yinqing, 2001. Fluid inclusions of the Dongping gold telluride deposit in Hebei province, China: Involvement of mantle fluid in metallogenesis. *Mineral Deposits*, 20(1): 23–36 (in Chinese with English abstract).

Mao Jingwen, Zhang Zhaochong, Yang Jianmin, Zuo Guochao, Zhang Zuoheng, Ye Dejin, Wang Zhiliang, Ren Fengshou, Zhang Yujun, Peng Cong, Liu Yuzhou and Jiang Mei, 2003. *The Metallogenic Series and Prospecting Assessment of Copper, Gold, Iron and Tungsten Polymetallic Ore Deposits in the West Sector of the Northern Qilian Mountains*. Beijing: Geological Publishing House, 157–242 (in Chinese).

Maynard, J.B., and Okita, P.M., 1991. Bedded barite deposits in the United States, Canada, Germany and China two major types based on tectonic setting. *Econ. Geol.*, 86: 364–376.

Niu Shuyin, Hou Quanlin, Hou Zengqian, Sun Aiquan, Wang Baode, Li Hongyang and Xu Chuanshi, 2003. Cascaded evolution of mantle plumes and metallogenesis of core- and mantle-derived elements. *Acta Geologica Sinica* (English Edition), 77(4): 522–536.

No. 8 Geological Party of the Xinjiang Bureau of Geology and Mineral Exploration and Development, 1994. *Inspecting and Appraising Report of the Bulong Gold Deposit in Aheqi County, Xinjiang*. 58 (unpublished) (in Chinese).

No. 8 Geological Party of the Xinjiang Bureau of Geology and Mineral Exploration and Development, 1999. *Geological Reconnaissance Survey Report of the Bulong Gold Deposit in Aheqi County, Xinjiang*, 53 (unpublished) (in Chinese).

Radtke, A.S., Rye, R.O., and Dickson, F.W., 1980. Geology and stable isotope studies of the Carlin gold deposit, Nevada. *Econ. Geol.*, 75: 641–672.

Romberger, S.B., 1986. Ore deposits 9, disseminated gold deposits. *Geosci. Canada*, 13(1): 27–32.

Stuart, F.M., Burnard, P.G., Taylor, R.P., and Turner, G., 1995. Resolving mantle and crustal contribution to ancient hydrothermal fluids: He-Ar isotopes in fluid inclusions from Dae Hwa W-Mo mineralisation, South Korea. *Geochim. Cosmochim. Acta*, 59: 4663–4673.

Urabe, T., and Sato, T., 1978. Kuroko deposits of the Kosaka mine, Northeast Honshu, Japan-products of submarine hot springs on Micocene seafloor. *Econ. Geol.*, 73: 161–179.

Wang Denghong and Mao Jingwen, 1996. Advances in the studies of helium isotopes geology. *Geol. Sci. Technol. Inf.*, 15(2): 51–56 (in Chinese with English abstract).

Wang Denghong, 1996. Sulfur and lead isotopic geochemistry of the Ashele volcanogenic massive sulfide deposit, Xinjiang, China. *Geochimica*, 25(6): 582–590 (in Chinese with English abstract).

Wang Denghong,Yu Jinjie, Yang Jianmin, Yan Shenghao, Xue Chunji and Chen Yuchuan, 2002. Inert gas isotopic studies and dynamic background of Cenozoic ore-forming process in China. *Mineral Deposits*, 21(2): 179–186 (in Chinese with English abstract).

Wang Weiping, 2001. Characteristics of aeromagnetic field and metallogenic prognosis of Wuqia-Keping area, southwestern part of Tianshan. *Uranium Geol.*, 17(3): 162–167 (in Chinese with English abstract).

Wang, Z.C., and Li, G.Z., 1991. Barite and witherite deposits in Lower Cambrian shales of south China: Stratigraphic distribution and geochemical characterization. *Econ. Geol.*, 86: 354–363.

Wu Chaodong, Yang Chengyun and Chen Qiying, 1999. The hydrothermal sedimentary genesis of barite deposits in west Hunan and east Guizhou. *Acta Scientiarum Naturalium Universitatis Pekinensis*, 35(6): 774–785 (in Chinese with English abstract).

Xiao Long, Wang Fangzheng, Fu Minlu, Begg, G. and Hayward N., 2001. Hydrothermal alteration and oreforming fluids evolution of the Jingxi-Yelmend gold deposit, Xinjiang, China. *Acta Geologica Sinica* (Chinese edition), 75(4): 518–526 (in Chinese with English abstract).

Xu Wenyi, Ren Qijiang, Xu Zhaowen, Fang Changquan, Guo Guozhang and Zhang Zhongze, 1997. Numerical modeling of evolution of ore-forming fluid in the Zijinshan copper-gold deposit, Fujian province. *Mineral Deposits*, 16(2): 163–169 (in Chinese with English abstract).

Xu Yongchang, Shen Ping, Tao Mingxin and Liu Wenhui, 1996. Geochemistry of mantle-derived volatile in the natural gases of eastern petroleum and gas fields: Ⅰ. New type of helium resources: industrial accumulation of mantle-derived helium in the sedimentary strata. *Sci. China* (D), 26(1): 1–8 (in Chinese).

Xu Yongchang, Shen Ping, Liu Wenhui, Tao Mingxin, Sun Mingliang and Du Jianguo, 1998. *Geochemistry of Rare Gas in the Natural Gases*. Beijing: Science Press, 99 (in Chinese).

Yang Fuquan, Ye Qingtong, Fu Xujie and Ye Jinhua, 1999. Distribution and metallogenic conditions of gold deposits in Southwest Tianshan Mountains. *Xinjiang Geol.*, 17(2): 129–136 (in Chinese with English abstract).

Yang Fuquan and Wu Hai, 1999. Geological characteristics and genesis of Bulong gold deposit in Xinjiang. *Bulletin of the 562 Comprehensive Geol. Brigade, Chinese Acad. Geol. Sci.*, 14: 60–68 (in Chinese with English abstract).

Yao Zhongyou, 1994. A preliminary discussion on geological characteristics and genesis of the Laerma gold deposit in Luqu county, Gansu province. *Mineral Deposits*, 13(1): 19–27 (in Chinese with English abstract).

Ye Qingtong, Fu Xijie and Zhang Xiaohua, 1997. Geological characteristics and genesis of the Ashele copper-zinc massive sulfide deposit, Xinjiang. *Mineral Deposits*, 16(2): 97–106 (in Chinese with English abstract).

Ye Qingtong, Wu Yiping, Fu Xujie, Chen Mingyong, Ye jinhua, Zhuang Daoze, Yang Fuquan and Bai Honghai, 1999. *Ore-forming Conditions and Metallogenic Prognosis of Gold and Nonferrous Metallic Resources in Southwestern Tianshan Mountains*. Beijing: Geological Publishing House, 70–93 (in Chinese with English abstract).

Ying Hanlong, 1999. The global background of epithermal gold deposits. *J. Precious Metallic Geol.*, 8(4): 241–250 (in Chinese with English abstract).

Ying Hanlong, 2001. Characteristics and origin of the Carlin-type gold deposits. *Geol.-Geochem.*, 29(4): 56–64 (in Chinese with English abstract).

Yu Jinjie, Hou Zengqian and Qu Xiaoming, 2001. Origin of high ^{18}O ore forming fluids in Gacun Kuroko deposit. *Acta Petrol. Mineral.*, 19(4): 382–389 (in Chinese with English abstract).

Zhang Dequan, Li Daxing, Zhao Yiming, Chen Jinghe, Li Zilin and Zhang Keyao, 1991. The Zijinshan deposit: the first example of quartz-alunite type epithrmal deposits in the continent of China. *Geol. Rev.*, 37(6): 481–491 (in Chinese with English abstract).

Zhang Dequan, She Hongquan, Li Daxing and Feng Chengyou, 2003. The porphyry-epithermal metallogenic system in the Zijinshan region, Fujian province. *Acta Geologica Sinica* (Chinese edition), 77(2): 253–261 (in Chinese with English abstract).

Zhang Fuxin, Zong Jingting and Ma Jianqin, 1998. A tentative discussion on the Carlin-type gold deposits in Qinling and related problems. *Mineral Deposits*, 17(2): 172–184 (in Chinese with English abstract).

Zhang Lianchang, Shen Yuanchao, Li Houmin, Zeng Qingdong, Li Guangming and Liu Tieing, 2002. Helium and argon isotopic compositions of fluid inclusions and tracing to the source of ore-forming fluids for Jiaodong gold deposits. *Acta Petrol. Sinica*, 18(4): 559–565 (in Chinese with English abstract).

Zheng Minghua, Liu Jiajun and Long Xunrong, 1996. *Ore-forming Geological Conditions and Target Study of Muruntau-type Gold Deposit in Southern Tianshan Mountains, Xinjiang*. 29–42 (unpublished) (in Chinese).

Zheng Yongfei and Chen Jiangfeng, 2000. *Stable Isotope Geochemistry*. Beijing: Science Press, 218–247 (in Chinese).